

# Magnetotransport in nanostructures: the role of inhomogeneous currents

Tiago S. Machado<sup>1</sup>, M. Argollo de Menezes<sup>2</sup>, Tatiana G. Rappoport<sup>3</sup>, and Luiz C. Sampaio<sup>1</sup>

<sup>1</sup>*Centro Brasileiro de Pesquisas Físicas, Xavier Sigaud,  
150, Rio de Janeiro, RJ, 22.290-180, Brazil*

<sup>2</sup>*Instituto de Física, Universidade Federal Fluminense,  
Rio de Janeiro, RJ, 24.210-346, Brazil and*

<sup>3</sup>*Instituto de Física, Universidade Federal do Rio de Janeiro,  
Rio de Janeiro, RJ, 68.528-970, Brazil*

(Dated: October 31, 2018)

## Abstract

In the study of electronic transport in nanostructures, electric current is commonly considered homogeneous along the sample. We use a method to calculate the magnetoresistance of magnetic nanostructures where current density may vary in space. The current distribution is calculated numerically by combining micromagnetic simulations with an associated resistor network and by solving the latter with a relaxation method. As an example, we consider a Permalloy disk exhibiting a vortex-like magnetization profile. We find that the current density is inhomogeneous along the disk, and that during the core magnetization reversal it is concentrated towards the center of the vortex and is repelled by the antivortex. We then consider the effects of the inhomogeneous current density on spin-torque transfer. The numerical value of the critical current density necessary to produce vortex core reversal is smaller than the one that do not take the inhomogeneity into account.

## I. INTRODUCTION

Electric transport in magnetic nanostructures is a useful tool both for probing and for manipulating the magnetization. In the low current density regime, magnetoresistance curves are useful for probing the sample's magnetization state while, in the high current density regime, magnetization patterns can be modified by a spin-transfer torque [1–3]. Magnetoresistance measurements have the advantage of being relatively simple and fast, serving as an efficient magnetic reading mechanism [4, 5].

Depending on thickness and diameter, small ferromagnetic disks exhibit stable topological defects called magnetic vortices [6, 7]. These vortices can be manipulated by picosecond pulses of few (tens of) Oersted in-plane magnetic fields that switch their polarity [8–13], making them good candidates for elementary data storage units [9].

For their use as storage units, the most viable form of manipulation of the magnetization is through spin-torque transfer, with the injection of high density electrical currents [1]. The effect of these currents in the magnetization dynamics is described theoretically by the incorporation of adiabatic and non-adiabatic spin-torque terms in the Landau-Lifshitz-Gilbert (LLG) equation [14, 15]. These two terms are proportional to the injected current density and it is normally considered an homogeneous current distribution inside the disk. Although theoretical predictions using this approach agree qualitatively with experimental results, there is a lack of quantitative agreement between theoretical and experimental results regarding to the current densities necessary to modify the magnetic structures [17–19].

In this paper we investigate the effect of non-uniform current distributions on electronic transport and spin-torque transfer in ferromagnetic systems exhibiting vortices. We calculate numerically the magnetoresistance (MR) and local current distribution of a ferromagnetic disk by separating the timescales for magnetic ordering and electronic transport. We consider an effective anisotropic magnetoresistance (AMR) that depends on the local magnetization. We discretize the disk in cells and solve the Landau-Lifshitz-Gilbert (LLG) equation [20] numerically with fourth-order Runge-Kutta [21], obtaining the magnetization profile of the disk. This pattern is used to calculate the magnetoresistance of each cell as a fixed current  $I$  is applied at two symmetrically distributed electrical contacts, resulting in a voltage drop and an inhomogeneous current distribution along the disk.

This method couples the electric and magnetic properties of the metallic nanomagnets

and can be used to analyze the effect of inhomogeneous current distributions in different contexts. First, we discuss the limit of low current density where transport measurements can be used to probe the magnetic structure. We compare the magnetic structure with magnetoresistance curves and show how magnetoresistance measurements could be interpreted to obtain information on the magnetization profile and its dynamics during the vortex core magnetization reversal. Moreover, we discuss the consequences of a non-homogeneous current distribution on spin-torque transfer and find that the critical current density that produces vortex core reversal is reduced by one order of magnitude whenever such non-inhomogeneity is taken into account. This result can be seen as a new route to understand why experimental values of the critical current densities are usually lower than the ones obtained in LLG calculations [17–19].

This article is organized as follows: In section II we discuss the model and method for the calculation of the magnetoresistance and current distribution. In section III, we exemplify the calculations by considering the magnetoresistance and current distributions of a Permalloy disk exhibiting a magnetic vortex. In section IV, we study the consequences of a non-homogeneous current distribution on spin-torque transfer. In section V we summarize the main results.

## II. MAGNETORESISTANCE AND CURRENT DISTRIBUTION CALCULATIONS

Let us consider a 36nm-thick Permalloy disk with a diameter of 300 nm discretized into a grid of  $4 \times 4 \times 4\text{nm}^3$  cells. The dynamics of the magnetization vector associated with each cell is given by the Landau-Lifshitz-Gilbert equation, which we numerically integrate with fourth-order Runge-Kutta and discretization step  $h = 10^{-4}$  [21]. The parameters associated with the LLG equation are the saturation magnetization  $M_s = 8.6 \times 10^5 \text{A/m}$ , exchange coupling  $A = 1.3 \times 10^{-11} \text{J/m}$  and Gilbert damping constant  $\alpha = 0.05$  [13].

By varying the external in-plane magnetic field  $H$  from negative to positive saturation we obtain a hysteresis curve, as depicted in Fig. 1, which is consistent with experimental observations [7]. As shown in Fig. 1(a), in static equilibrium and in the absence of magnetic fields, a vortex structure with a core magnetized perpendicular to the disk plane is formed in the center of the disk. If a small in-plane magnetic field  $H$  is applied, the core is displaced

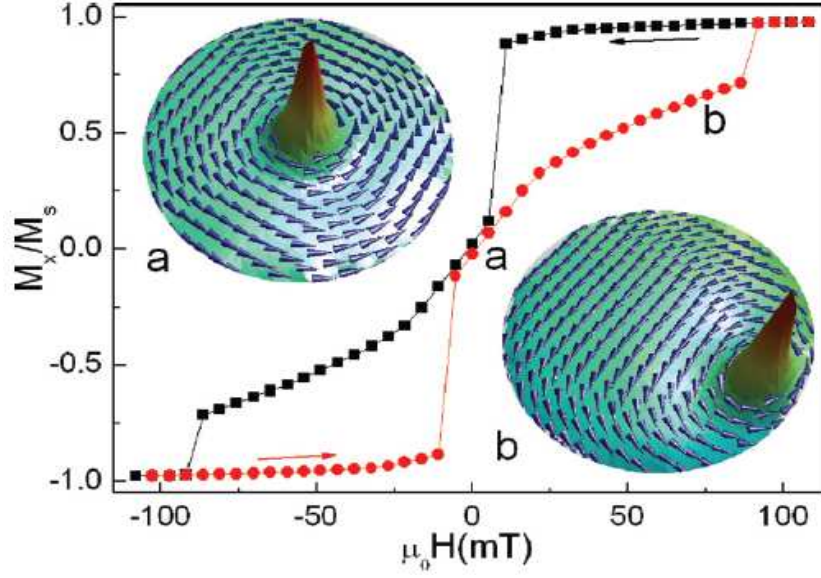


FIG. 1: Magnetic hysteresis obtained with micromagnetics simulation of a Py disk with a diameter of 300 nm and thickness of 36 nm subject to a static, in-plane magnetic field  $H$ . Two configurations for the vortex core, corresponding to different external fields (0 and 75 mT), are also depicted.

from the center (Fig. 1(b)). At a critical field  $H_{c1}$  the vortex is expelled from the disk, resulting in a discontinuity in the hysteresis loop. As the external field  $H$  is lowered back, the vortex structure reappears, but at a lower field  $H_{c2} < H_{c1}$ .

In order to investigate the electronic transport on the nanomagnetic disk we consider the magnetization profile  $\{\vec{M}_i\}$ , obtained as the stationary solution of the LLG equation, as a starting point to calculate the magnetoresistance  $R_i$  in each cell  $i$  of the disk. It is well established that in relatively clean magnetic metals the main source of magnetoresistance is the anisotropic magnetoresistance (AMR) [22], which can be expressed as  $\rho = \rho^\perp + (\rho^\parallel - \rho^\perp)\cos^2\phi$ , where  $\phi$  is the angle between the local magnetization and the electric current and  $\rho^\perp$  and  $\rho^\parallel$  are the resistivities when the magnetization is perpendicular and parallel to the current, respectively. We decompose the current into orthogonal components  $x$  and  $y$  such that if the normalized projection of the magnetization  $\vec{M}_i$  on the current direction  $\hat{u}$  ( $u = x, y$ ) is  $m_i^u = \cos\phi$ , and the cell geometrical factor is taken into account, the magnetoresistance  $R_i$  is split into orthogonal components as  $R_i^u = R_i^\perp + (R_i^\parallel - R_i^\perp)(m_i^u)^2$  in every cell  $i$  of the disk (Fig. 2). Thus, we obtain a resistor network where the resistances depend on the local magnetization and are assumed to be approximately constant at the

time scale of electronic scattering processes.

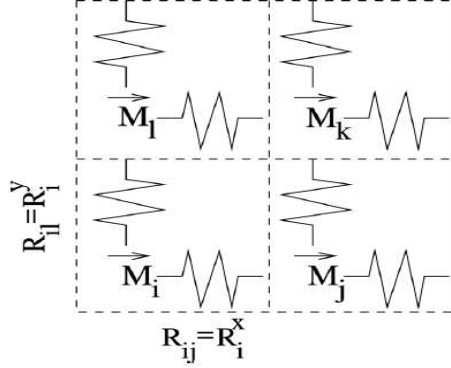


FIG. 2: Original cells used in the LLG simulation with the associated resistance network.

Guided by recent experiments [23] we allow a constant current  $I$  to flow along the disk by attaching symmetrically placed electrodes on it (see Fig. 3). The voltage drop along the resistors and the associated current map of the disk are obtained by solving Kirchoff's equation iteratively at each node of the grid with a relaxation method [24, 25]:

$$V_i^{(n+1)} = \left( \sum_{\langle j \rangle} 1/R_{ij} \right)^{-1} \left( \sum_{\langle j \rangle} \frac{V_j^{(n)}}{R_{ij}} + b_i \right), \quad (1)$$

where  $R_{ij}$  is  $R_i^x$  ( $R_i^y$ ) if  $i$  and  $j$  are horizontal (vertical) neighbors and  $b_i$  is the boundary current, assumed to be  $I$  ( $-I$ ) at the leftmost (rightmost) cells and zero otherwise (see Fig. 2).  $V_i^n$  is the voltage at site  $i$  after  $n$  iterations and the sums run over the nearest-neighbors  $\langle j \rangle$  of node  $i$ . Starting with a random initial condition  $\{V_i^{(0)}\}$  at each site we iterate Eq.1 until each  $V_i^{(n)}$  becomes stationary (within 9 decimal digits precision). After convergence we calculate the equivalent resistance, the ratio  $R_{eq} = \Delta V/I$  between the voltage drop  $\Delta V$  between the electrodes, given by

$$\Delta V = \sum_{i||b_i=I} V_i - \sum_{j||b_j=-I} V_j, \quad (2)$$

and the current  $I$  entering the disk.

### III. MAGNETO-STRUCTURE AND MAGNETORESISTANCE

#### A. Hysteresis and magnetoresistance

In order to obtain the magnetoresistance curves, the calculation discussed in the previous section is performed at different fields. Magnetoresistance and current distribution for the same points of the hysteresis loop in Fig. 1 are depicted in Fig. 3. Fig. 3(a) displays magnetoresistance curves for both homogeneous (without using the resistance network [26]) and non-homogeneous current distributions. The vortex expulsion and its formation at a different critical field are clearly identified and, with  $\rho^{\parallel} = 155\Omega\cdot\text{nm}$  and  $\rho^{\perp} = 150\Omega\cdot\text{nm}$ , we obtain a MR of 1.2% for the non-homogeneous distribution, which is a typical value found in experiments [23, 27].

One also observes that magnetoresistance curves for uniform and non-uniform current distributions differ significantly, the latter being more comparable to experimental results with same contact geometry [23]. As expected, a homogeneous current overestimates the magnetoresistance, since the current will flow thru regions of high resistance, whereas if the current found by solving Laplace's equation on the associated resistor network, one finds a preferential path (higher current density) on regions of low resistance. This difference is more pronounced in the presence of a vortex, since the magnetization of the disk is highly non-homogeneous on such configuration.

In the light of the discussion above, one sees in Fig. 3 (b)-(c) that the current is not homogeneously distributed inside the disk, being stronger towards the center of the vortex core. In the center of the disk the magnetization either points in  $\hat{z}$  direction, perpendicular to the direction of current flow, or loops about the vortex core. In both cases, the current has a path where its direction is always perpendicular to the magnetization, reducing the local magnetoresistance. Above the saturation field, the magnetization is uniform and at the disk center the same happens to the current. The red (blue) region has a current density 1 – 2% larger (smaller) than the current  $I$  at saturation. This effect might be enhanced if other sources of magnetoresistance are considered, as giant magnetoresistance for example. Similar approaches, using different sources of magnetoresistance and geometries had been used to calculate the magnetoresistance in nanomagnets [27–32].

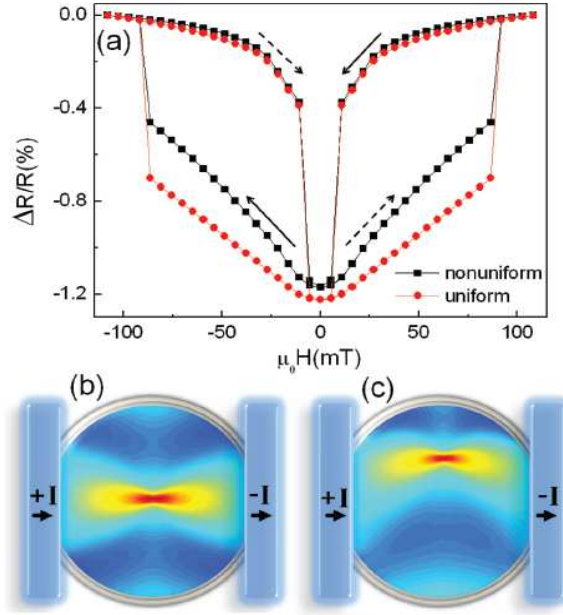


FIG. 3: (a) Magnetoresistance for the magnetic configurations obtained in Fig 1 for uniform (circle) and non-uniform (square) current distribution. Bottom: electric current map for (b) zero field and (c)  $H = 75 \text{ mT}$ . The red (blue) color corresponds a current density which is about 1 – 2% larger (smaller) than the uniform current at the saturation field.

## B. Dynamics

Next, we study the dynamics of the vortex core magnetization reversal by the application of short in-plane magnetic fields. Under a pulsed in-plane magnetic field or spin polarized current excitation, the vortex with a given polarity ( $V^+$ ) dislocates from the center of the disk with nucleation of a vortex ( $V^-$ )-antivortex ( $AV^-$ ) pair with opposite polarity after the vortex attains a critical velocity of rotation about the disk center [3, 33]. The original  $V^+$  then annihilates with the  $AV^-$ , and a vortex with reversed core magnetization ( $V^-$ ) [9] remains. If a low-density electronic current is made to flow through the sample (without disturbing the magnetization dynamics), we observe changes in the magnetoresistance, as the vortices nucleate and annihilate. We depict in Fig. 4(a) the dynamics of the magnetoresistance as a pulsed, in-plane magnetic field is applied in the  $\hat{x}$  direction at  $t = 20 \text{ ps}$  for different pulse intensities. The pulses have their shape sketched in grey in Fig. 4(a) with full width at half maximum of  $t=250 \text{ ps}$ . Depending on the pulse intensity, the vortex core

magnetization does not reverse at all ( $\mu_0 H < 43$  mT), reverses once ( $54 \text{ mT} < \mu_0 H < 64$  mT) or multiple times ( $\mu_0 H > 64$  mT) [12, 13].

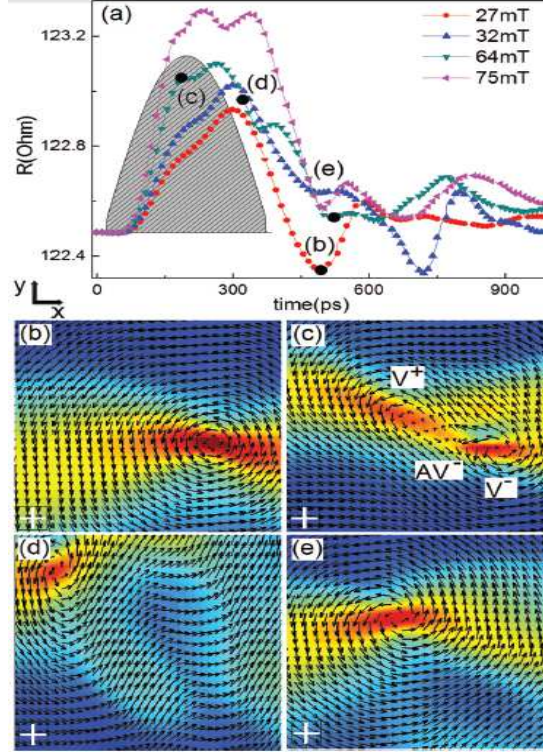


FIG. 4: (a) Evolution of magnetoresistance after the application of pulsed, in-plane magnetic fields (the shape is shown in grey) with different intensities. Snapshots of magnetization (arrows) and current distribution (color map) for pulse fields without (b) and with (c)-(e) vortex core magnetization reversal. The white cross shows the position of the disk center. Both current and magnetic field are applied in the  $\hat{x}$  direction

During the application of a field pulse in the  $\hat{x}$  direction, i.e., parallel to the current flow, the vortex core is pushed to the  $\hat{y}$  direction breaking the rotation symmetry of the disk's magnetization, increasing both the total  $m_x$  component and the disk's equivalent resistance (see Fig. 4(a)). At  $t = 340$  ps the field is practically zero and, from the decay of magnetoresistance to its equilibrium (initial) value, one can infer whether there was reversal of the vortex core polarization or not: for pulses that induce reversal, the value of the magnetoresistance just after the pulse is always larger than its initial value. If there is no reversal the magnetoresistance attains a minimum value that is lower than its initial value, i.e., before the application of the pulse, and oscillates about it.

In Figs. 4(b)-(e) we depict snapshots of current (color map) and magnetization (arrows) distributions at time steps marked with black dots in Fig. 4(a), in situations with or without vortex core magnetization reversal. Whenever the pulse decreases its intensity, the total  $m_x$  component and the equivalent resistance of the disk follow the same pattern (although with some time delay), because the vortex core tends to return to the disk center, where  $m_x = 0$ . Panel (b) shows the current distribution and magnetization at a moment corresponding to the minimum of the resistance curve, for a field intensity  $\mu_0 H = 27mT$ , for which there is no vortex core reversal. There is a large region with  $m_y$  magnetization (and small  $m_x$ ) in the center of the disk. This region, together with the vortex core, creates a low resistance path for the electronic current, decreasing the equivalent resistance towards a value below the equilibrium resistance. Panels (c), (d) and (e) show magnetization and current distributions at different moments of the vortex core magnetization reversal for a situation where there is a single reversal ( $\mu_0 H = 64mT$ ). In panel (c) we depict the current distribution at the exact moment of nucleation of the  $V^-AV^-$  pair, the initial stage of vortex core magnetization reversal. Panel (d) shows the spin waves emitted just after the  $V^+AV^-$  annihilation, a process that occurs with energy dissipation. Such energy loss drives the vortex core to the disk center along with some small oscillations, mainly due to reflections of spin waves at the edges of the disk. It turns out that the resistance follow equivalent behavior: it decreases towards the initial resistance value and remains always above it. Panel (e) shows the current distribution after the field pulse has vanished. As can be seen, the time dependent resistance curves can give us an indication of the vortex reversal process.

Let us discuss in further details the interplay between magnetization pattern and current distribution. In Fig. 5 (a) we show a snapshot of the current distribution during the vortex core magnetization reversal process, with the  $V^+$  and the  $V^-AV^-$  pair with negative polarity. As shown in Figs. 3, 4 and 5(b) the current is pushed to the vortex core, where  $m_x = 0$  and, consequently, the local resistance is minimum. With the nucleation of the  $AV^-$  vortex (Fig. 5 (a)),  $m_x$  gets larger than zero around it, with  $m_y \rightarrow 0$ . As current flows in the  $\hat{x}$  direction, it is *repelled* from the antivortex core.

In the latter analysis we considered a particular orientation of the AV. However, as can be seen in Figs. 5(c) and (d), depending on their orientation, antivortices can either attract (in the first case) or repel currents (in the latter case). Vortices are rotation invariant, and always attract current towards their cores. It is important to point out that this difference in current

distributions might have important consequences in the high-density current spin-torque transfer acting on either a vortex or an antivortex. For instance, although the inversion process through spin-torque for an AV is equivalent to the one for a V, we should expect different current densities in each one, since currents can only penetrate the AV core at a particular orientation.

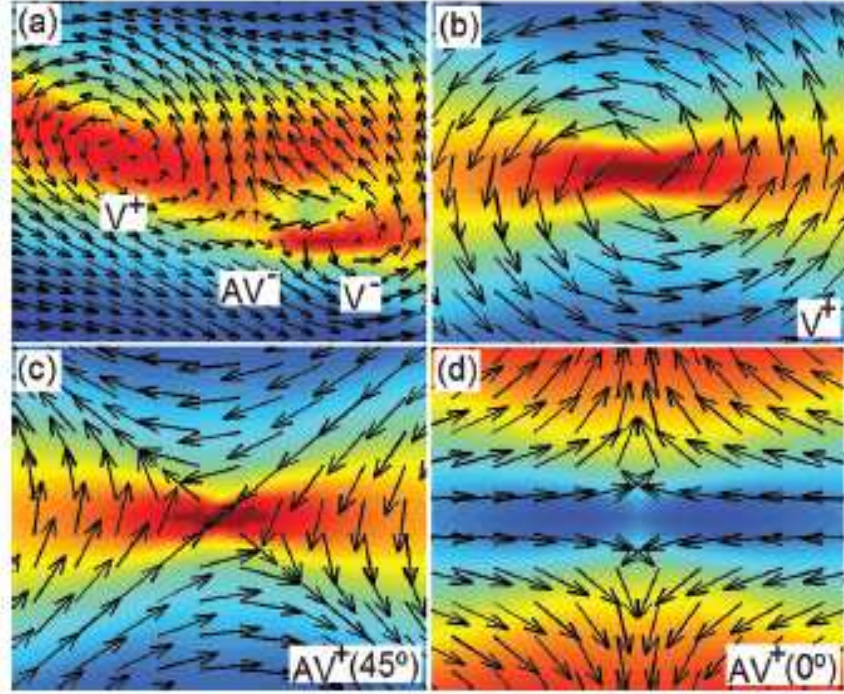


FIG. 5: (a)-(d) Snapshots of magnetization (arrows) and current distribution (color map) of (a) the vortex core magnetization reversal process at  $t = 214$  ps, (b) a vortex and its associated current distribution, and (c)-(d) antivortices rotated by 45 degrees with respect to each other and their associated current distribution. Depending on the relative orientation of the antivortex it can either focus (c) or repel (d) currents away from the center of the core.

#### IV. SPIN-TORQUE TRANSFER

In this section, we discuss the consequences of inhomogeneous currents in the spin-torque transfer. In order to check how the current distribution is incorporated in the spin-torque terms of the modified LLG equation, we need to review a few steps of their derivations. It is important to note that in our approach, the only source of non-homogeneous current

distribution is the anisotropic magnetoresistance, as discussed in section II. All other effects are neglected.

The itinerant electrons spin operator satisfies the continuity equation

$$\frac{d}{dt}\langle \mathbf{s} \rangle + \nabla \cdot \langle \hat{\mathbf{J}} \rangle = -\frac{i}{\hbar}(\langle [\mathbf{s}, H] \rangle) \quad (3)$$

where  $\hat{\mathbf{J}}$  is the spin current operator. The Hamiltonian  $H$  is the s-d Hamiltonian ( $H_{sd} = -J_{ex}\mathbf{s} \cdot \mathbf{S}$ ), where  $\mathbf{s}$  and  $\mathbf{S}/S = -\mathbf{M}/M_s$  are the spins of itinerant and localized electrons, and  $J_{ex}$  is the exchange coupling strength between them. We define spin current density  $\mathbf{J} = \langle \hat{\mathbf{J}} \rangle = -(g\mu_B P/eM_s)\mathbf{j}_e(\mathbf{r}) \otimes \mathbf{M}$ , where  $\mathbf{j}_e(\mathbf{r})$  is the current density, and the electron spin density is given by  $\mathbf{m} = \langle \mathbf{s} \rangle$ [14]. We use the same approximations, previously used to calculate the spin-torque [14, 15], with the new ingredient of non-homogeneous current density. We obtain

$$\begin{aligned} \frac{d}{dt}\mathbf{m} = & \frac{\mu_B P}{eM_s} [\mathbf{M}(\nabla \cdot \mathbf{j}_e(\mathbf{r})) + (\mathbf{j}_e(\mathbf{r}) \cdot \nabla)\mathbf{M}] \\ & - \frac{J_{ex}S}{M_s}\mathbf{m} \times \mathbf{M}, \end{aligned} \quad (4)$$

where,  $\mathbf{M}$  is the matrix magnetization,  $g$  is the Landé factor splitting,  $\mu_B$  is the Bohr magneton,  $P$  is the spin current polarization of the ferromagnet,  $e$  is the electron charge. From the continuity equation for charges, the term containing  $\nabla \cdot \mathbf{j}_e(\mathbf{r})$  is always zero, even if the current density is not constant. As discussed previously, the same divergent is used to determine the current distribution in section II. This expression is exactly the same expression obtained previously but with  $\mathbf{j}_e(\mathbf{r})$  in the second term of the right side of the equation varying with  $\mathbf{r}$ . This current distribution is introduced at the modified LLG that considers spin-torque transfer. Therefore, we obtain a spin-torque transfer where the current distribution is not uniform.

To consider spin-torque transfer effects we include adiabatic and non-adiabatic spin torque terms in the LLG equation,

$$\begin{aligned} \frac{d}{dt}\mathbf{m} = & -\gamma_0\mathbf{m} \times \mathbf{H}_{eff} + \alpha\mathbf{m} \times \frac{d}{dt}\mathbf{m} \\ & -(\mathbf{u} \cdot \nabla)\mathbf{m} + \beta\mathbf{m} \times [(\mathbf{u} \cdot \nabla)\mathbf{m}], \end{aligned} \quad (5)$$

where,  $\mathbf{m}=\mathbf{M}/M_s$  is the normalized local magnetization,  $\alpha$  is a phenomenological damping constant,  $\gamma_0$  is the gyroscopic ratio,  $\mathbf{H}_{eff}$  is the effective field, which is composed of the applied external field, the demagnetization field, the anisotropy field and the exchange field. The first term describes the precession of the normalized local magnetization about the

effective field. The second term describes the relaxation of the normalized local magnetization and  $\beta$  is a dimensionless parameter that describes the strength of the non-adiabatic term, which we consider to be 0.5 [15, 16]. The velocity  $\mathbf{u}(\mathbf{r}) = (gP\mu_B/2eM_s)\mathbf{j}_e(\mathbf{r})$  is a vector pointing parallel to the direction of electron flow and  $\mathbf{j}_e(\mathbf{r})$  is calculated using the procedure discussed in section II.

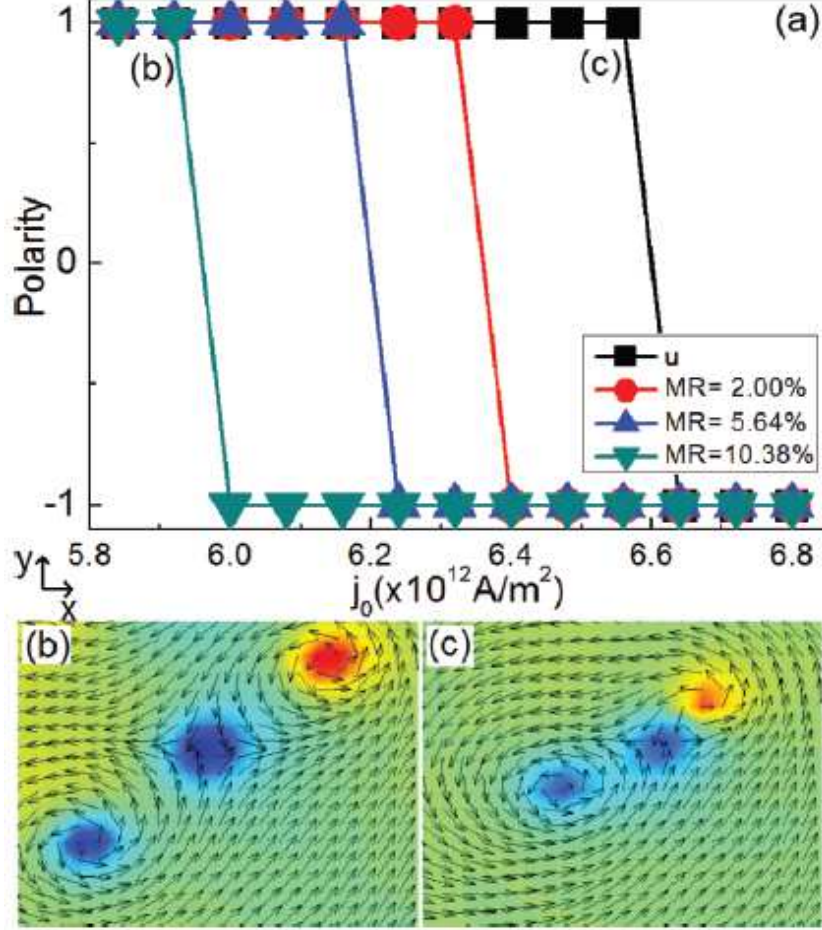


FIG. 6: (a): Core polarity as a function of current density for homogeneous (squares) and non-homogeneous current distributions (with different MR). (b) and (c): magnetization profiles during the inversion process at the critical current for both non-homogeneous (b) and homogeneous (c) current distributions. The color map represent the out-of-plane magnetization,  $m_z$ , and the arrows represent the in-plane component.

To explain the importance of our assumption about the current distribution let us analyze the critical current density  $\mathbf{j}_e^c$ , the minimal current density needed to produce a vortex core

reversal. For this purpose, we simulated the magnetization dynamics of a system subjected to a DC current with the modified LLG equation (equation 5). In Fig. 6(a) one sees the vortex core polarity as a function of current density  $\mathbf{j}_e$ . The different curves represent situations of homogeneous current (squares) and of three different values of AMR where the magnetoresistance ranges from 2% to 10%. Such AMR, as discussed in the previous sections, shape the degree of current inhomogeneity throughout the disk. One can see that the critical current density  $\mathbf{j}_e^c$  in our model is 3 – 10% smaller than the one obtained for uniform currents. These results suggest a new route, together with the non-adiabatic term, to explain the discrepancy between experimental results and theoretical calculations of the critical current density  $\mathbf{j}_e^c$ .

Our analysis might also have important technological implications, since we observe a (almost linear) correlation between the current density necessary to produce a core inversion and the anisotropic magnetoresistance of the material. Thus, by increasing the AMR of the sample, one can decrease the critical current  $\mathbf{j}_e^c$ , which is strongly desirable in memory devices for the sake of low energy consumption and minimal heat waste.

Panels (b) and (c) of Fig. 6 show the magnetic configurations for the moment just before the  $V^+$ - $AV^-$  annihilation, at the critical current density, for the model with non-homogeneous and homogeneous current distributions, respectively. In the case of inhomogeneous currents, the fact that a  $V(AV)$  attracts (*repels*) the current affects the velocity and separation distance of the  $V$ - $AV$  pair during the vortex core reversal. As antivortices *repel* currents, the current density at their core is smaller, making them slower than vortices. As a result, after the nucleation of the  $V^-$ - $AV^-$  pair their separation occurs faster than in the case where the current density in the center of a  $V$  or an  $AV$  is the same, as usually considered in micromagnetic simulations.

## V. CONCLUSIONS

We performed a realistic calculation of magnetoresistance effects in magnetic nanostructures subject that takes into account inhomogeneous current densities. For that purpose, we adapted a numerical relaxation scheme for the Laplace equation to the solution of the LLG equation for the magnetization profile along a Permalloy disk. Our results suggest that resistance measurements might be useful to probe the dynamics of vortex core mag-

netization reversal, induced by short in-plane magnetic pulses. Moreover, we note that the difference between current distributions close to vortices and anti-vortices have significant consequences for the spin-torque transfer effect. The inhomogeneous current distribution inside the magnet reduces substantially the critical current density necessary to produce a vortex core reversal. We conclude that materials with large anisotropic magnetoresistance need lower current densities to modify their magnetic structure, a much desirable feature for most modern memory devices.

### Acknowledgements

This work was supported by CNPq and FAPERJ. LCS and TGR acknowledge the “INCT de Fotônica” and “INCT de Informação Quântica”, respectively, for financial support.

- 
- [1] J. C. Slonczewski, J. Magn. Magn. Mater. **159**, L1 (1996); L. Berger, Phys. Rev. B **54**, 9353 (1996).
  - [2] D. C. Ralph, M. D. Stiles, J. Magn. Magn. Mater **320**(7), 1190 (2008).
  - [3] K. Yamada, S. Kasai, Y. Nakatani, K. Kobayashi, H. Kohno, A. Thiaville, T. Ono, Teruo, Nat. Mater. **6**, 269 (2007).
  - [4] I. N. Krivorotov, N. C. Emley, J. C. Sankey, S. I. Kiselev, D. C. Ralph, R. A. Buhrman, Science **307**,215 (2005).
  - [5] S. Choi, K. -S. Lee and S. -K. Kim, Appl. Phys. Lett. **89**, 062501 (2006).
  - [6] T. Shinjo, T. Okuno, R. Hassdorf, K. Shigeto, and T. Ono, Science **289**, 930 (2000).
  - [7] R. P. Cowburn, D. K. Koltsov, A. O. Adeyeye, M. E. Welland, and D. M. Tricker, Phys. Rev. Lett. **83**, 1042 (1999).
  - [8] M. Weigand, B. Van Waeyenberge, A. Vansteenkiste, M. Curcic, V. Sackmann, H. Stoll, T. Tylliszczak, K. Kaznatcheev, D. Bertwistle, G. Woltersdorf, C. H. Back, and G. Schutz, Phys. Rev. Lett. **102**, 077201 (2009).
  - [9] A. Vansteenkiste, K. W. Chou, M. Weigand, M. Curcic, V. Sackmann, H. Stoll, T. Tylliszczak, G. Woltersdorf, C. H. Back, G. Schtz, and B. Van Waeyenberge, Nature **5**, 332 (2009).
  - [10] B. Van Waeyenberger, A. Puzic, H. Stoll, K. W. Chou, T. Tylliszczak, R. Hertel, M. Fahnle,

- H. Bruckl, K. Rott, G. Reiss, I. Neudecker, D. Weiss, C. H. Back, and G. Schutz, *Nature* **444**, 461 (2006).
- [11] R. Hertel, S. Gliga, M. Fähnle, and C. M. Schneider, *Phys. Rev. Lett.* **98**, 117201 (2007).
- [12] S. K. Kim, K. S. Lee, Y. S. Yu, and Y. S. Choi, *Appl. Phys. Lett.* **92**, 022509 (2008); K. S. Lee, K. Y. Guslienko, J. Y. Lee, and S. K. Kim, *Phys. Rev. B* **76**, 174410 (2007).
- [13] T. S. Machado, T. G. Rappoport, and L. C. Sampaio, *Appl. Phys. Lett.* **93**, 112507 (2008).
- [14] S. Zhang, and Z. Li, *Phys. Rev. Lett.* **93**, 127204 (2004).
- [15] A. Thiaville, Y. Nakatani, J. Miltat, and Y. Suzuki, *Europhys. Lett.* **69**, 990 (2005)
- [16] L. Heyne, J. Rhensius, D. Ilgaz, A. Bisig, U. Rudiger, M. Klau, L. Joly, F. Nolting, L. J. Heyderman, J. U. Thiele, and, F. Kronast, *Phys. Rev. Lett.* **105**, 187203 (2010).
- [17] K. Yamada, S. Kasai, Y. Nakatani, K. Kobayashi, and T. Ono, *Appl. Phys. Lett.* **93**, 152502 (2008).
- [18] K. Yamada, S. Kasai, Y. Nakatani, K. Kobayashi, and T. Ono, *Appl. Phys. Lett.* **96**, 192508 (2010).
- [19] G. S. D. Beach, M. Tsoi and J.L. Erskine, *J. Magn. Magn. Mater.* **320** 1272 (2008).
- [20] T.L. Gilbert, *Physical Review*, **100** 1243 (1955).
- [21] W.H. Press, B.P. Flannery, B.P. Teukolsky, S.A. Vetterling and T. William, *Numerical Recipes in C: The Art of Scientific Computing*(Cambridge University Press, 1992).
- [22] R. C. O’Handley, *Modern Magnetic Materials* (Wiley-Interscience, New York, 1999), Chap. 15.
- [23] S. Kasai, Y. Nakatani, K. Kobayashi, H. Kohno, and T. Ono, *Phys. Rev. Lett.* **97**, 107204 (2006).
- [24] R. Courant, K. Friedrichs, and H. Lewy, *Phys. Math. Ann.* **100**, 32 (1928).
- [25] H. Gould and J. Tobochnik, *An Introduction to Computer Simulation Methods* (Addison-Wesley, 1996), Chap. 10.
- [26] R. A. Silva, T. S. Machado, G. Cernicchiaro, A. P. Guimaraes, and L. C. Sampaio, *Phys. Rev. B*, **79**, 134434 (2009).
- [27] P. Vavassori, M. Grimsditch, V. Metlushko, N. Zaluzec, and B. Ilic, *Appl. Phys. Lett.* **87**, 072507 (2005).
- [28] H. Li, Y. Jiang, Y. Kawazoe, and R. Tao, *Phys. Lett. A* **298**, 410-415 (2002).
- [29] M. Bolte, M. Steiner, C. Pels, M. Barthelmess, J. Kruse, U. Merkt, G. Meier, M. Holz, and

- D. Pfannkuche, Phys. Rev. B **72**, 224436 (2005).
- [30] M. Holz, O. Kronenwerth, and D. Grundler, Phys. Rev. B **67**, 195312 (2003).
- [31] Jun-ichiro Ohe, S. E. Barnes, Hyun-Woo Lee, and S. Maekawai, Appl. Phys. Lett. **95**, 123110 (2009)
- [32] L. K. Bogart and D. Atkinson, Appl. Phys. Lett. **94**, 042511 (2009)
- [33] K. Y. Guslienko, K. S. Lee, and S. K. Kim, Phys. Rev. Lett. **100**, 027203 (2008).